Beamforming and Transceiver HW Design for THz Band

Mubarak Umar Aminu[*], Oskari Tervo[†], Janne Lehtomäki[*], and Markku Juntti[*]
[*]Centre for Wireless Communications, University of Oulu, P.O.Box 4500, FI-90014 University of Oulu, Finland
Email: {firstname.lastname}@oulu.fi
[†]Nokia Bell Labs, Oulu, Finland Email: oskari.tervo@nokia-bell-labs.com

Abstract—The new spectrum available in the millimeter-wave (mmWave) and Terahertz (THz) bands is a promising frontier for the future wireless communications. Propagation characteristics at these frequencies imply that highly directional transmissions should be used to focus the available power to a specific direction. This is enabled by using tightly packed large-scale antenna arrays to form narrow or so called pencil beams both at the transmitter and the receiver. This type of communication is, however, quite sensitive to imperfections of the transceivers, resulting in beam pointing errors and lost connection in the worst-case. This paper investigates the impact of such errors, originating from the local oscillators in terms of phase noise, which is a major impairment with high center frequencies. We explore the impact of these effects with different transceiver architectures, illustrate the beam shape properties, and quantify their impact on the system performance for different modulation schemes in terms of error rates. Specifically, we model the phase noise both as Wiener and Gaussian distributed to characterize the impact of phase noise on the beam accuracy and system performance.

I. INTRODUCTION

The number of wireless devices and required data rates are expected to grow at an unprecedented rate in the upcoming years. This has led to the conclusion that the existing LTE spectrum and the associated techniques cannot fulfill the requirements, but more spectrum is needed. Thus, the first standards of 5G are especially interested in new bands between 6-30 GHz (cmWaves) and 30-100 GHz (mmWaves), but even higher frequencies up to and above 300 GHz (THz) have been identified as a potential frontier in the future [1], [2]. A particularly attractive feature in the higher frequencies is the huge available contiguous bandwidth, which enables very short symbol intervals, and, thus, extreme data rates. However, there are many challenges which need to be resolved in order to implement such systems.

A major challenge is drastically increased propagation attenuation, which needs to be overcome by highly directional transmission with large antenna arrays by forming narrow beams to get the signal propagate a reasonable distance. These beams can be formed using different transceiver architectures, but so far, the most promising approaches are either fully analog beamforming, hybrid beamforming with small number of RF chains, or hybrid/fully digital beamforming with low-resolution digital-to-analog converters due to their lower complexity [3]–[6]. The first one applies only low-complexity analog phase shifters to adjust the beam direction in addition to electromagnetically directive antenna elements, while the other ones use also digital processing to enhance the beamforming capability. They can also enable spatial multiplexing.

Another important challenge with high central frequencies is the phase noise (PN) caused by local oscillators (LOs) in the frequency up-conversion and down-conversion phase at the transmitter and receiver, respectively. As the term suggest, phase noise causes random changes in the observed carrier phase of the signal, and it increases significantly with the carrier frequency [7], [8]. The impact of phase noise on the communication is that it causes the receiver to sample the signal in a wrong time instant, resulting in rotation of the symbols in the constellation and consequently leading to symbol errors. This phase variation may be compensated for up to some extent, but it becomes more and more challenging when the beams become narrower and the symbol interval decreases.

In many prior works, free-running oscillators are assumed and the phase noise has been modeled as a Wiener process with Gaussian distributed increments between each sampling instant. Depending on the implementation, the impact of phase noise can be different [9] in multi-antenna systems. In particular, phase noise can be correlated or even fully uncorrelated between different radio frequency (RF) chains depending on the transceiver architecture and implementation. In the correlated case, there is a common LO shared among the RF chains and all the chains experience the same rotation. The phase noise is uncorrelated when each RF chain is equipped with independent LO.

In this paper, we study the impact of phase noise in a multi-antenna hybrid architecture. We investigate the effects of phase noise to the beam properties with different LO architectures at the transmitter. We model the phase noise using different correlation models to approximate different LO architectures and evaluate their impact on the communications performance. We study the cases of common LO shared among all the RF chains, and independent LO for each RF chain. We consider a multi-carrier orthogonal frequency-division multiplexing (OFDM) system using coherent and non-coherent modulation schemes. In OFDM systems, the phase noise generally results in a common phase error (CPE) to all the subcarriers and inter-carrier interference (ICI) that is different for all the subcarriers [10], [11]. We analyze how the phase noise affects the system performance in terms of signal constellation and bit error rate (BER). We specifically

compare how the impact of phase noise from correlated and uncorrelated sources on the coherent quadrature phase shift keying (QPSK) and differentially coherent QPSK (DQPSK).

II. SYSTEM MODEL

We consider a multi-antenna system with one transmitter and one receiver as shown in Fig. 1. The transmitter has
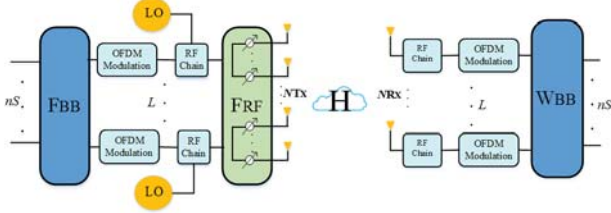

Fig. 1. Hybrid transmitter and fully digital receiver.

a hybrid architecture with N_{Tx} transmit antennas and $L \leq N_{\text{Tx}}/M$ RF chains, where M is the number of antennas per each subarray. The receiver is equipped with a fully digital architecture with N_{Rx} antennas. We assume a multi-carrier OFDM transmission with K subcarriers and N_s data streams. At the transmitter, the information bits are first modulated into constellation symbols (either QPSK or DQPSK) and then mapped to N_s streams, where we assume $N_s = L$ and $L \leq N_{\text{Rx}}$. Let $\mathbf{D} = \begin{bmatrix} \mathbf{D}_1, \ldots, \mathbf{D}_{ns} \end{bmatrix}$ denote the N_s data streams, where $\mathbf{D}_i$ is the i-th stream. The N_s symbol streams are then loaded onto the RF chains by applying a digital precoder $\mathbf{F}_{\text{BB}} \in \mathbb{C}^{L \times N_s}$, i.e., $\mathbf{S} = \begin{bmatrix} \mathbf{S}_1, \ldots, \mathbf{S}_L \end{bmatrix} = \mathbf{F}_{\text{BB}}\mathbf{D}$. Using a serial-to-parallel converter, the precoded symbols $\{\mathbf{S}_l | l = 1, 2, \ldots, L\}$ are converted into length-K signals $\begin{bmatrix} \mathbf{S}_l[0], \mathbf{S}_l[1], \ldots, \mathbf{S}_l[K-1] \end{bmatrix}$. The frequency-domain OFDM signal is then converted into the time-domain OFDM symbols $\begin{bmatrix} s_l[0], s_l[1], \ldots, s_l[K-1] \end{bmatrix}$ by taking the inverse Fourier transform i.e.,

$$s_l[m] = \frac{1}{\sqrt{K}} \sum_{k=0}^{K-1} S_l[k] e^{\left(j2\pi mk/K\right)}. \tag{1}$$

A cyclic prefix (CP) is added to the time-domain OFDM symbol and then up-converted to the RF in L RF chains respectively, and then fed into the subarrays that further use phase shifters for analog precoders. The transmitted OFDM symbol at the RF front end now becomes

$$\mathbf{x}[m] = \mathbf{F}_{\text{RF}}\mathbf{s}[m], \tag{2}$$

where $\mathbf{F}_{\text{RF}} \in \mathbb{C}^{N_{\text{Tx}} \times L}$ is block-diagonal i.e., it is implemented using a partially connected network of phase shifters and can be represented as

$$\mathbf{F}_{\text{RF}} = \begin{bmatrix} \mathbf{F}_{\cdot,1}^{\text{RF}} & 0 & \cdots & 0 \\ 0 & \mathbf{F}_{\cdot,2}^{\text{RF}} & \cdots & 0 \\ \vdots & \cdots & \ddots & \vdots \\ 0 & \cdots & \cdots & \mathbf{F}_{\cdot,l}^{\text{RF}} \end{bmatrix}$$

where $\mathbf{F}_{\cdot,l}^{\text{RF}} \in \mathbb{C}^{M \times 1}$ is the phase shifter weight vector for each RF chain. The transmitted vector $\mathbf{x}[m]$ propagates through the channel $\mathbf{h}[m] \in \mathbb{C}^{N_{\text{Tx}} \times N_{\text{Rx}}}$ and is received at the receiver by N_{Rx} antennas. At the receiver, the signal is down-converted to baseband and after removing the CP, the received time domain OFDM symbol can be expressed as

$$\mathbf{y}[m] = \mathbf{h}[m] \odot \mathbf{F}_{\text{RF}}\mathbf{s}[m] + \mathbf{v}[m], \tag{3}$$

where $\mathbf{v}[m]$ is the time-domain complex Gaussian noise, $\odot$ denotes circular convolution and $\mathbf{y}[m] \in \mathbb{C}^{N_{\text{Rx}} \times 1}$ is the received vector with elements $\begin{bmatrix} y_1[m], y_2[m], \ldots, y_{N_{\text{Rx}}}[m] \end{bmatrix}$. The frequency-domain signal $\mathbf{Y}[k] = \begin{bmatrix} Y_1[k], \ldots, Y_{N_{\text{Rx}}}[k] \end{bmatrix} \in \mathbb{C}^{N_{\text{Rx}} \times 1}(k = 0, 1, \ldots, K - 1)$ can be obtained by taking the Fourier transform. The frequency-domain signal $Y_{n_{\text{r}}}[k]$ can therefore be written as

$$Y_{n_{\text{r}}}[k] = \sum_{m=0}^{K-1} y_{n_{\text{r}}}[m] e^{\left(-j2\pi mk/K\right)}. \tag{4}$$

III. PHASE NOISE MODEL

A. Influence of Phase Noise

Phase noise originates from local oscillators at the transmitter during up-conversion to the RF frequency and at the receiver during the down-conversion to the baseband. The phase noise introduced by these oscillators essentially means that not all the power is concentrated on the single desired frequency, but spreads around the center frequency. This equals to jitter in time domain. To introduce the influence of the phase noise in the baseband, the time domain signal at the transmitter is multiplied by $e^{\theta_l[m]}$. The transmitted OFDM symbol (2) therefore becomes

$$\mathbf{x}[m] = \mathbf{F}_{\text{RF}}\mathbf{\Theta}[m]\mathbf{s}[m], \tag{5}$$

where $\mathbf{\Theta}[m] \in \mathbb{C}^{L \times L}$ is a diagonal matrix, whose entries are $\{e^{\theta_l[m]} | l = 1, 2, \ldots, L\}$ the phase noise components for each RF chain. The phase noise is modeled as a Wiener process, i.e.,

$$\theta_l[m] = \theta_l[m-1] + w_l[m], \tag{6}$$

where $w_l[m]$ is a complex Gaussian random variable. Note that, the phase noise $\{e^{\theta_l[m]} | l = 1, 2, \ldots, L\}$ among the different RF chains depends on the LO architecture. When all the RF chains are driven by a common LO, the phase noise components $\{e^{\theta_l[m]} | l = 1, 2, \ldots, L\}$ are the same, i.e., fully correlated. In the case where each RF chain is driven by an independent LO, the phase noise of different RF chains can be considered as fully uncorrelated. In this paper, we consider the impact of phase noise originating from the LO at the transmitter only. The received time-domain OFDM symbol with the effect of the phase noise can be expressed as

$$\mathbf{y}[m] = \mathbf{h}[m] \odot \mathbf{F}_{\text{RF}}\mathbf{\Theta}[m]\mathbf{s}[m] + \mathbf{v}[m]. \tag{7}$$

In the frequency-domain, the received signal at the n_r-th antenna and k-th subcarrier $Y_{n_\mathrm{Rx}}[k]$ with the effect of the phase noise now becomes [12]

$$
\begin{aligned}
Y_{n_\mathrm{r}}[k] &= \frac{1}{\sqrt{K}} \sum_{m=0}^{K-1} y_{n_\mathrm{r}}[m] e^{\left(-j2\pi mk/K\right)} \\
&= \sum_{m=0}^{K-1} \left(\mathbf{h}_{n_\mathrm{r}}[m] \odot \mathbf{F}_{\mathrm{RF}}\boldsymbol{\Theta}[m]\mathbf{s}[m] + \mathbf{n}[m]\right) e^{\left(-j2\pi mk/K\right)} \\
&= \sum_{m=0}^{K-1} \sum_{n_\mathrm{t}=1}^{N_\mathrm{Tx}} h_{n_\mathrm{r},n_\mathrm{t}}[m] \odot \sum_{l=1}^{L} F_{n_\mathrm{t},l}^{\mathrm{RF}} e^{j\theta_l[m]} s_l[m] e^{\left(-j2\pi mk/K\right)} \\
&\quad + \sum_{m=0}^{K-1} v_{n_\mathrm{r}}[m] e^{\left(-j2\pi mk/K\right)} \\
&= \sum_{n_\mathrm{t}=1}^{N_\mathrm{Tx}} \sum_{p=0}^{K-1} H_{n_\mathrm{r},n_\mathrm{t}}[p] \sum_{l=1}^{L} F_{n_\mathrm{t},l}^{\mathrm{RF}} \phi_l[k-p] S_l[p] + V_{n_\mathrm{r}}[k] \\
&= \sum_{n_\mathrm{t}=1}^{N_\mathrm{Tx}} \sum_{l=1}^{L} \phi_l[0] H_{n_\mathrm{r},n_\mathrm{t}}[k] F_{n_\mathrm{t},l}^{\mathrm{RF}} S_l[k] + V_{n_\mathrm{r}}[k] \\
&\quad + \sum_{n_\mathrm{t}=1}^{N_\mathrm{Tx}} \sum_{p=0,p\neq k}^{K-1} H_{n_\mathrm{r},n_\mathrm{t}}[p] \sum_{l=1}^{L} F_{n_\mathrm{t},l}^{\mathrm{RF}} \phi_l[k-p] S_l[p], \quad (8)
\end{aligned}
$$

where $\phi_l(k) = \frac{1}{K} \sum_{m=0}^{K-1} e^{j\theta_l[m]} e^{\left(-j2\pi mk/K\right)}$. In a more compact form, the received frequency domain vector can be expressed as

$$
\mathbf{Y}[k] = \boldsymbol{\Phi}[0]\mathbf{H}[k]\mathbf{F}_{\mathrm{RF}}\mathbf{S}[k] + \mathbf{I}_{\mathrm{ICI}}[k] + \mathbf{V}[k]. \quad (9)
$$

where $\boldsymbol{\Phi}[0] = \mathrm{diag}\big(\phi_1(k),\ldots,\phi_L(k)\big) \in \mathbb{C}^{L\times L}$ and $\mathbf{I}_{\mathrm{ICI}}[k] = \left[I_1^{\mathrm{ICI}}[k],\ldots,I_{N_\mathrm{Rx}}^{\mathrm{ICI}}[k]\right] \in \mathbb{C}^{N_\mathrm{Rx}\times 1}$ and $I_{n_\mathrm{r}}^{\mathrm{ICI}}[k]$ is defined as $I_{n_\mathrm{r}}^{\mathrm{ICI}}[k] = \sum_{n_\mathrm{t}=1}^{N_\mathrm{Tx}} \sum_{p=0,p\neq k}^{K-1} H_{n_\mathrm{r},n_\mathrm{t}}[p] \sum_{l=1}^{L} F_{n_\mathrm{t},l}^{\mathrm{RF}} \phi_l[k-p] S_l[p]$.

From (9) we can observe that the received signal is affected by the phase noise in two ways. The first is the multiplication of the signal by a complex number in the first term in (9). It causes rotation of the desired signal. The effect is common and appears across all subcarriers and is termed as the common phase error (CPE). The second effect in the additive term $\mathbf{I}_{\mathrm{ICI}}[k]$ which leads to inter-carrier-interference (ICI). This implies that the orthogonality between the subcarriers is lost due to the phase noise effect.

IV. NUMERICAL RESULTS AND ANALYSIS

In this section, we analyze the impact of phase noise using computer simulations. We begin by analyzing the impact of phase noise to the beam properties. To do so, we consider line of sight scenario and operating frequency of 100 GHz. The transmitter is equipped with $N_\mathrm{Tx} = 32$ antennas and $L = 8$ RF chains. The transmitter directs the beam towards the receiver located at $33°$. We evaluate the error between the ideal main lobe magnitude and the main lobe magnitude with the phase noise, i.e., $EVM = |AF_\mathrm{PN} - AF_\mathrm{ideal}|^2 / |AF_\mathrm{ideal}|^2$ where AF is the array factor calculated as

$$
AF_\mathrm{PN}(\varphi) = |(\mathbf{F}_\mathrm{RF}\boldsymbol{\Theta}[m]\mathbf{s})^H \mathbf{a}(\varphi)|^2,
$$

where $\mathbf{a}(\varphi) = [1, e^{i2\pi r_2 \sin(\varphi)/\lambda}, \ldots, e^{i2\pi r_N \sin(\varphi)/\lambda}]^T$ and φ is the direction of departure, r_n is the distance between the n_Tx-th element and the first element, and λ is the wavelength. The simulations are performed by assuming a correlation model between the RF chains (as shown in Fig. 2) so that the
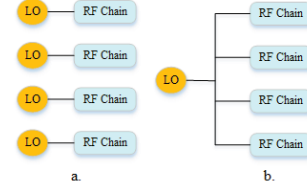

Fig. 2. LO architectures.

phase noise samples are generated from multivariate Gaussian distribution $\mathcal{N}(\mathbf{0}, \Sigma)$, where zero-vector $\mathbf{0}$ is the mean and Σ is the $L \times L$ covariance matrix which can be written as

$$
\Sigma = \begin{bmatrix} \sigma^2 & \cdots & \rho \\ \vdots & \ddots & \vdots \\ \rho & \cdots & \sigma^2 \end{bmatrix},
$$

where ρ is the correlation coefficient and σ^2 is the element-wise variance. The correlation coefficient ρ takes value either 0 or 1, i.e., $\rho = 0$ means the phase noise between the corresponding RF chain is uncorrelated when $\rho = 1$ the phase noise is correlated.

The impact of the phase noise on the beam response is shown in Fig. 3. In the figure, we plotted the beam response for different values of the phase noise variance i.e., $\sigma^2 = [1°, \ldots, 7°]$. The phase noise when modelled as a Wiener process leads to a significant increase in the side lobe levels and beam pointing errors as can be seen in Fig. 3(b) and Fig. 3(c). The impact is less severe when the phase noise is modelled as Gaussian. We noticed that the phase noise has no impact on the beam pattern, when the phase noise across the RF chains are fully correlated, i.e., have common LO among the RF chains (Fig. 3(d)).

The main lobe magnitude error, beam pointing error, side lobe level are shown in Figs. 4, 5 and 6, respectively. All the plots are averaged over 10000 simulation runs. As shown in Fig. 4, the main lobe magnitude deviates more as the phase noise variance increases when the phase noise is uncorrelated among the RF chains. This same trend is observed in the beam pointing error as shown in Fig. 5. The beam deviates as much as $6°$ from the ideal beam direction with a phase noise variance of $10°$. Fig. 6 shows the side lobe level due to the phase noise. From the plots we can see that the phase noise increases the error more, when it is generated by uncorrelated sources. Also when the phase noise is Gaussian the performance is better compared to when the phase noise is from Wiener process.

To investigate the impact of the phase noise in the baseband, we performed a system level simulations, in which we have considered a MIMO-OFDM system. The transmitter employs a hybrid beamforming with $N_\mathrm{Tx} = 32$ antennas and $L = 4$ RF

(a) PN as Gaussian   (b) PN as WP (10 symbols)   (c) PN as WP (20 symbols)   (d) $\rho = 1$ WP (20 symbols)
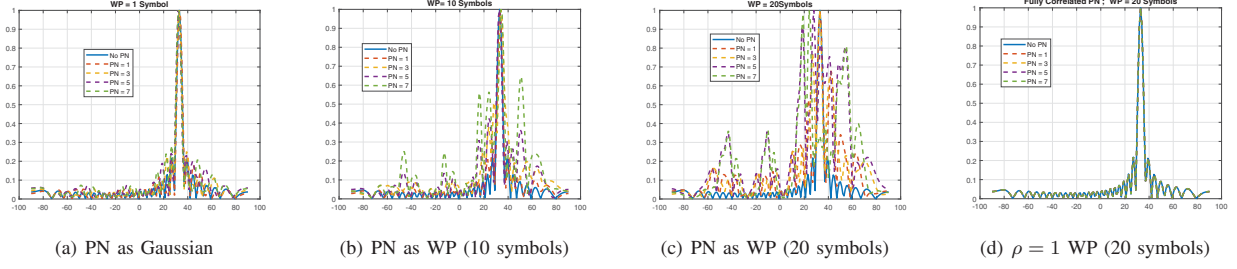
Fig. 3. Antenna beam pattern in the presence of phase noise for different numbers of symbols over which phase noise accumulates before synchronization.
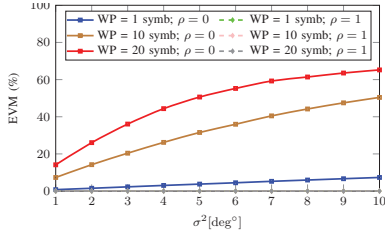

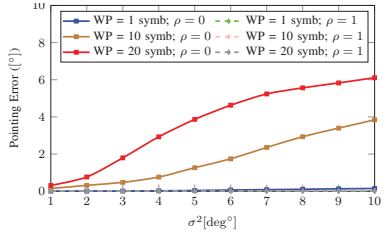Fig. 4. Antenna main lobe EVM vs. phase noise variance.

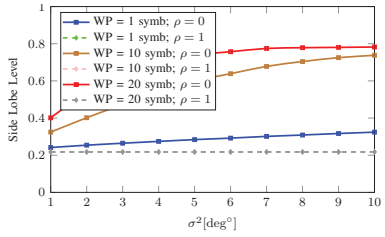Fig. 5. Antenna main beam pointing error vs. phase noise variance.

Fig. 6. Relative antenna side lobe level vs. phase noise variance.

chains and we set the number of data streams $N_s = L$. The receiver is fully digital with $N_{\text{Rx}} = 32$ antennas. We compare QPSK and DQPSK. We assume scattering environment with a LoS and 2 nonLoS path and we assume knowledge of the channel $\mathbf{H}$ at the transmitter and it remains unchanged for several OFDM symbols. The hybrid beamformers $\mathbf{F}_{\text{RF}}$ and $\mathbf{F}_{\text{BB}}$ are designed based on the channel. Figs. 7 and 8 show the constellation diagram for the QPSK and DQPSK, respectively. The phase noise variance for all the plots is $3°$ and the SNR is 20 dB. The combination of the two effects (CPE and ICI) on the constellation caused by the phase noise can be noticed.

From the plots, we can see the effects of the phase noise when it is uncorrelated among the RF chains and when it is fully correlated in both QPSK and DQPSK. Comparing Fig. 7(a) and Fig. 7(b), it can be seen that the uncorrelated phase noise i.e., $\rho = 0$ causes clouds in the constellation (some additive white Gaussian like noise) which is the ICI. This implies that uncorrelated phase noise have more severe impact on the orthogonality of the subcarriers which may be destroyed if the phase noise is large. In the case where the phase noise is fully correlated among the RF chains i.e., $\rho = 1$, the phase noise causes some phase jitter in the constellation as shown in Fig. 7(b). We can also observe the effect of the phase noise when it is Gaussian and when it from a Wiener process. From Fig. 7(c) and Fig. 7(d) we can notice the rotation in the constellation when the phase noise is modeled as a Wiener process. The plot indicates that when the phase noise is from a Wiener process (whether correlated or uncorrelated) it causes CPE to the subcarriers. From Fig. 8(c) and Fig. 8(d), however, we can see that for the DQPSK even when the phase noise is from a Wiener process there is no rotation in the constellation. This shows that DQPSK is more robust to the CPE than the QPSK as expected and well-known. In Figs. 9 and 10, we plotted the BER vs. the phase noise variance. From the two figures, we can see that the DQPSK scheme is robust to the phase noise from correlated sources as shown in Fig. 10. The QPSK suffers from phase noise with both correlated and uncorrelated sources. When the phase noise is from a Wiener process the performance degrades in terms of BER for both modulation schemes.

V. CONCLUSION

In this paper, we studied the impact of phase noise in a multi-antenna hybrid transceiver architecture. We investigated the effects of phase noise to the beam properties and quantify their impact on the system performance for different modulation schemes. We modeled the phase noise from Gaussian distribution and Wiener process and using different correlation models to approximate different LO architectures. We studied the cases of common LO shared among all the RF chains, and the case of independent LO for each RF chain. We also considered an OFDM system using coherent and non-coherent modulation schemes. We then compared the impact of phase
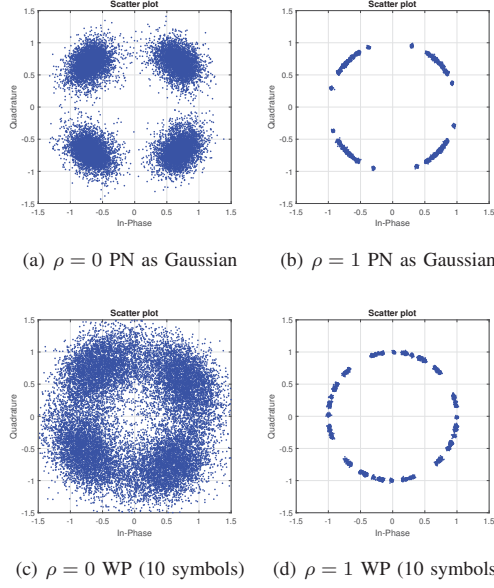
(a) $\rho = 0$ PN as Gaussian   (b) $\rho = 1$ PN as Gaussian

(c) $\rho = 0$ WP (10 symbols)   (d) $\rho = 1$ WP (10 symbols)

Fig. 7. QPSK constellation under PN.

(a) $\rho = 0$ PN as Gaussian   (b) $\rho = 1$ PN as Gaussian

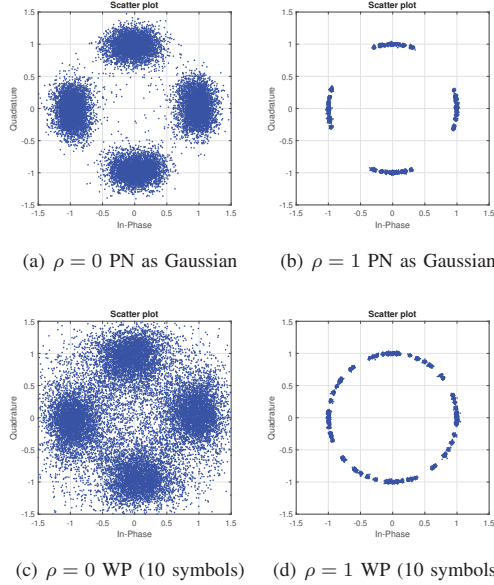(c) $\rho = 0$ WP (10 symbols)   (d) $\rho = 1$ WP (10 symbols)

Fig. 8. DQPSK constellation under PN.

noise from correlated and uncorrelated sources on the coherent QPSK and DQPSK schemes.
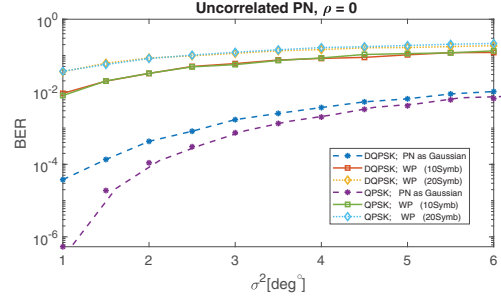
VI. Acknowledgment

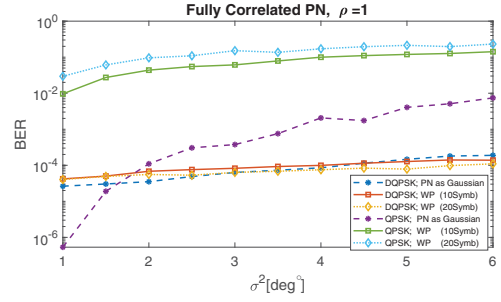Fig. 9. BER vs. phase noise variance $\rho = 0$

Fig. 10. BER vs. phase noise variance $\rho = 1$

References

[1] K. M. S. Huq, J. M. Jornet, W. H. Gerstacker, A. Al-Dulaimi, Z. Zhou, and J. Aulin, "THz communications for mobile heterogeneous networks," *IEEE Commun. Mag.*, vol. 56, no. 6, pp. 94–95, 2018.

[2] T. S. Rappaport, S. Sun, R. Mayzus, H. Zhao, Y. Azar, K. Wang, G. N. Wong, J. K. Schulz, M. Samimi, and F. Gutierrez, "Millimeter wave mobile communications for 5G cellular: It will work!" *IEEE access*, vol. 1, pp. 335–349, 2013.

[3] V. Desai, L. Krzymien, P. Sartori, W. Xiao, A. Soong, and A. Alkhateeb, "Initial beamforming for mmwave communications," in *Asilomar Conference on Signals, Systems and Computers, 2014 48th*. IEEE, 2014, pp. 1926–1930.

[4] A. Alkhateeb, J. Mo, N. Gonzalez-Prelcic, and R. W. Heath, "MIMO precoding and combining solutions for millimeter-wave systems," *IEEE Commun. Mag.*, vol. 52, no. 12, pp. 122–131, 2014.

[5] A. F. Molisch, V. V. Ratnam, S. Han, Z. Li, S. L. H. Nguyen, L. Li, and K. Haneda, "Hybrid beamforming for massive MIMO: A survey," *IEEE Commun. Mag.*, vol. 55, no. 9, pp. 134–141, 2017.

[6] S. Han, I. Chih-Lin, Z. Xu, and C. Rowell, "Large-scale antenna systems with hybrid analog and digital beamforming for millimeter wave 5G," *IEEE Commun. Mag.*, vol. 53, no. 1, pp. 186–194, 2015.

[7] H. Mehrpouyan, M. R. Khanzadi, M. Matthaiou, A. M. Sayeed, R. Schober, and Y. Hua, "Improving bandwidth efficiency in E-band communication systems," *IEEE Commun. Mag.*, vol. 52, no. 3, pp. 121–128, 2014.

[8] P. Smulders *et al.*, "Exploiting the 60 GHz band for local wireless multimedia access: prospects and future directions," *IEEE Commun. Mag.*, vol. 40, no. 1, pp. 140–147, 2002.

[9] H. Thomas, V. Ranki *et al.*, "Phase noise in beamforming," *IEEE Trans. Wireless Commun.*

[10] D. Petrovic, W. Rave, and G. Fettweis, *IEEE Trans. Commun.*

[11] S. Wu and Y. Bar-Ness, "OFDM systems in the presence of phase noise: consequences and solutions," *IEEE Trans. Commun.*

[12] Y.-P. Zhang, J. Liu, S. Feng, and P. Zhang, "Pilot design for phase noise mitigation in millimeter wave mimo-ofdm systems," in *IEEE 85th Vehicular Technology Conference (VTC Spring), 2017*. IEEE, 2017, pp. 1–6.